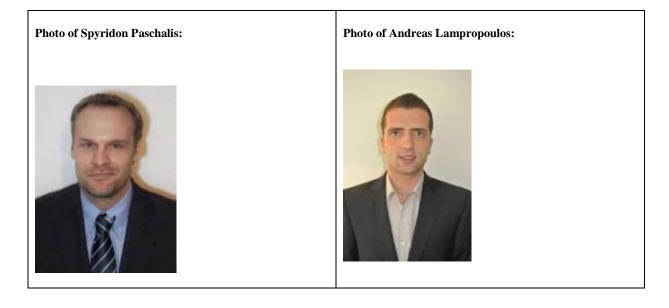
- 1 Fiber content and curing time effect on the tensile characteristics of Ultra
- 2 High Performance Fiber Reinforced Concrete (UHPFRC)
- 3 Spyridon A. Paschalis, Andreas P. Lampropoulos



- 5 University of Brighton, School of Environment and Technology,
- 6 Moulsecoomb, Brighton, BN2 4GJ, UK, E-mail:
- 7 S.paschalis@brighton.ac.uk
- 9 Running Head: Fiber content and curing time effect on UHPFRC

8

4

Abstract

Ultra High Performance Fiber Reinforced Concrete (UHPFRC) is a concrete type with superior mechanical properties and of a relatively high tensile strength. The tensile stress-strain characteristics of UHPFRC are highly affected by the mixture design and the curing regime. In the present study, an extensive experimental investigation has been conducted with direct tensile tests on a number of specimens that contained different percentages of steel fibers and different cement types were applied. Also, various curing regimes were investigated. Different models depending on the steel fiber amount were proposed for the simulation of the stress-strain and the stress-crack opening response of UHPFRC, while the fracture energy was also calculated for the different fiber contents. Finally, the effect of fiber content and curing time on the variation of the experimental results are discussed.

23 Keywords

- 24 UHPFRC, Direct Tensile Test, Fiber Content, Heat Curing, Stress-strain characteristics,
- 25 Fracture Energy

26 1. Introduction

Ultra High Performance Fiber Reinforced Concrete (UHPFRC) is a material which is characterized by enhanced properties in tension and compression and high energy absorption in the post-cracking state. The behavior of the material, especially in tension, is highly depended on the amount of fibers in the matrix and on the properties of the cementitious matrix. The ultimate strength in tension depends on the effectiveness and orientation of the fibers. When the post-cracking resistance is lower than the resistance of the matrix, strainsoftening occurs. If on the other hand, the post-cracking resistance of UHPFRC is higher than the resistance of matrix and the fibers can sustain a higher load after the formation of the first

35 crack then multiple cracks appear and this behavior is known as strain-hardening behavior [1]. This behavior normally characterizes the performance of UHPFRC at relatively high 36 fiber contents. The effect of different fiber contents on the tensile strength was investigated in 37 the present study through direct tensile tests, while the compressive behavior was evaluated 38 through standard compressive tests executed with cubes. 39 Another important parameter, which has been examined in the current study, is the effect of 40 curing time for different curing regimes on the compressive strength and the tensile stress-41 strain characteristics of UHPFRC. Hence, different curing conditions were applied for which 42 43 the performance of the material was determined. Finally, the effects of different percentages of steel fibers, and changing curing regimes on the variation of the experimental results were 44 studied. 45 Nicolaides et al. [2] presented an experimental work which was focused on the development 46 of Ultra High Performance Cementitious Composites locally available in Cyprus. Different 47 parameters that can affect the strength and the workability of UHPFRC were investigated in 48 49 their study and an optimum mixture was proposed. Kang et al. [3] and Yoo et al. [4] examined the effect of the steel fiber amount on the flexural 50 strength of UHPFRC and it was found that the flexural strength increased at increasing fiber 51 volume ratio, while the structural ductility was increased too. On the contrary, the post-peak 52 53 ductility at the softening region was decreased. Kang et al. [3] presented an inverse analysis 54 study to model the tensile fracture model of UHPFRC and a tri-linear tensile fracture model of UHPFRC tensile softening behavior was proposed. Another inverse finite element analysis 55 method was proposed by Neocleous et al. [5] for deriving the tensile characteristics of Steel 56 57 Fiber Reinforced Concrete (SFRC). Kooiman et al. [6] carried out inverse analysis and described a procedure for the development of a reliable bilinear stress-crack width model for 58 SFRC. 59

60 The orientation and distribution of the fibers in the mixture are important parameters affecting the mechanical properties of UHPFRC. Kang and Kim [7] investigated the effect of 61 the fiber orientation on the tensile behavior of UHPFRC. According to this study, the effect 62 of the fiber orientation on the pre-cracking behavior was found to be negligible, but it 63 significantly affected the post-cracking behavior. The importance of fiber distribution on the 64 performance of UHPFRC was also highlighted by Ferrara et al. [8]. In this study, the effect of 65 different fiber orientations was examined and it was found that the orientation of the fibers 66 affected the mechanical performance of the fiber reinforced cementitious composites. 67 68 Paschalis and Lampropoulos [9] investigated the size effect on the flexural performance of UHPFRC and it was found that as the depths of the prisms increased the flexural strength 69 decreased. The unique properties and the application of UHPFRC under monotonic and 70 71 cyclic loading in structural cases, where high mechanical properties are required, were 72 highlighted in a number of studies [10-14]. The superior performance of UHPFRC can be attributed to the enhanced tensile behavior. 73 74 However, until now, the effect of fibers and curing conditions on the tensile stress-strain behavior have not been investigated thoroughly. The present study focused on both aspects 75 76 and an extensive experimental investigation has been conducted with dog-bone shaped specimens tested in direct tension and standard cubes tested in compression. 77

2. Experimental Investigation

2.1 Materials and preparation

78

79

For the preparation of the specimens silica sand with a maximum particle size of 500µm was used together with dry silica fume with a retention on a 45 µm sieve of less than 1.5% and Ground Granulated Blast Furnace Slag (GGBS). Silica fume was used in order to increase the density of the matrix and to improve the rheological properties of the mixture. A low

84 water/cement ratio of 0.28 was applied together with polycarboxylate superplasticizer. The steel fibers had a length of 13 mm, a diameter of 0.16mm and a tensile strength of 3000 MPa 85 while the modulus of elasticity was 200 GPa. Two different cement types were used in the 86 87 present study, which were a high strength cement 52.5 N type I and a 32.5 R CEM II. The examined mixture (Table 1) was optimized in a previous study (Hassan et al. [15]) 88 The mixing procedure was as follows: the dry ingredients were mixed first for three minutes. 89

Then, water and superplasticizer were added in the mixture and once the mixture reached the

wet stage, steel fibers were added gradually through sieving.

2.2 Setup

90

91

92

93

94

95

96

97

98

99

100

101

102

103

104

105

106

In the present study and for the investigation of the performance of UHPFRC, different curing regimes and various fiber contents were tested; 76 dog bone specimens tested in tension and 64 standard cubes in compression; (4 samples per mixture). The geometry of the examined specimens is illustrated by Figure 1.

The tests were conducted using a servo-hydraulic testing machine. The extension was recorded using a Linear Variable Differential Transformer (LVDT) that was connected to a special steel frame; the displacement rate was 0.007 mm/sec (Figure 2a).

For the compressive tests, standard cubes with side lengths of 100 mm were used; the loading rate was 0.6 MPa/s, according to BS EN 12390-3:2009 [16]. The experimental setup of these tests is illustrated by Figure 2b.

2.3 Experimental results

2.3.1 Effect of the cement type

A preliminary study on the effect of cement type was conducted as a part of the current research. Two different types of cement were used (32.5 R type II and 52.5 N type I cement);

direct tensile tests were conducted in order to evaluate the tensile stress-strain characteristics and also compressive tests were executed. The percentage of steel fibers in the mixture for this investigation was 3% per volume. After demoulding (two days after the casting) the specimens were placed in a water curing tank for 26 days and tested after 28 days. The results of 6 dog-bone shaped specimens tested in tension and prepared with cement 32.5 R type II are illustrated in Figure 3a together with the average curve. The maximum tensile strength was 9.6 MPa and the modulus of elasticity was 53 GPa. The mean compressive strength of 4 standard cubes was 125.6 MPa. The respective results of the specimens prepared with cement class 52.5 N type I are presented by Figure 3b. The average maximum tensile strength of this mixture was 11.3 MPa, the modulus of elasticity was 56.2 GPa and the compressive strength was 150 MPa. A comparison of the average curves is presented by Figure 4. From the experimental results it is evident that due to the use of high strength cement a significant higher tensile strength of UHPFRC was obtained; the tensile strength of the specimens prepared with cement class 52.5 N type I was increased by 18% (Figure 4). Also, the compressive strength of UHPFRC increased by 16% when 32.5 R type II cement was replaced by 52.5 N type I cement. Based on these results and in order to achieve the optimum performance, cement 52.5 N type I was chosen for further investigation of the effect of different curing regimes and curing time on the performance of UHPFRC.

107

108

109

110

111

112

113

114

115

116

117

118

119

120

121

122

123

124

125

126

127

128

129

130

2.3.2 Effect of the curing regime on the tensile and compressive strengths of UHPFRC

Crucial parameters that affect the performance of UHPFRC are the curing regime and the curing duration. Heat curing is often applied for UHPFRC in order to accelerate the strength development. The present study focuses on the effect of the curing regime and curing

131 duration on the tensile stress-strain characteristics of UHPFRC. Nicolaides et al. [2] investigated the effect of different curing temperatures and concluded that the optimum 132 performance is achieved for a curing at 90 °C. This outcome also is in agreement with other 133 studies [17-18] and 90 °C was also adopted in the present study. 134 The specimens were demoulded 2 days after casting and some of the specimens were placed 135 in a water tank at a water temperature of 20 °C (±2 °C), while other specimens were steam-136 cured at 90 °C (±2 °C). Testing was conducted at 3, 7, 14 and 28 days, while further 137 investigation at 90 days took place for specimens cured in the water tank (Table 2). For this 138 139 part of study, high strength cement 52.5 N was used together with 3 % per volume steel fibers. The results of the direct tensile tests with the dog-bone shaped specimens for different 140 concrete ages and for different curing conditions are presented by Figures 5-9. 141 142 The development of the maximum tensile strength in time for the different curing conditions is presented by Figure 10. 143 From the stress-strain results summarized in Figure 10 it can be noticed that the tensile 144 strength of the UHPFRC specimens placed in a water curing tank increased rapidly during the 145 first 28 days, while after this period an increase of only 5.8% can be observed. For the 146 specimens cured in the steam curing tank on the other hand, there is a clear strength increase 147 during the first 14 days, while after this period the tensile strength remains almost constant. 148 Also, it can be noticed that the 14 days tensile strength of the steam-cured specimens is 149 150 almost the same as the 90 days tensile strength of specimens cured under normal curing conditions. 151 The compressive strength results for the different curing conditions are presented in the same 152 153 graph in Figure 11. The results of Figure 11 indicate an upward trend of the compressive strength at increasing 154 age for the specimens cured in the water tank during the 90 days period. When comparing the 155

results for different curing conditions, it can be observed that the 7 days strength of the steam-cured specimens is almost the same as the 90 days strength of the specimens cured under normal conditions, which indicates the effectiveness of the steam curing on the acceleration of the strength development. The maximum compressive strength was achieved for steam-cured specimens after 14 days while further curing did not significantly affect the compressive strength, which is comparable with the tensile behaviors.

2.3.3 Investigation of the effect of heat curing on the variation of the experimental

results

From the results presented in Figures 5-9 it is evident that there is a scatter of the experimental results, which can be attributed to differences in the distribution and orientation of the fibers and to the less developed bond strength between the fibers and the matrix. In order to quantify this effect, the Coefficient of Variation (CV), was calculated for the steam-cured specimens and the results are presented by Figure 12.

Figure 12 shows that the CV considerably decreases at increasing curing time. This reduction in the CV values and the subsequent reduction in the scatter of the experimental results can be attributed to the improvement of the strength of the concrete matrix at increasing curing time.

2.3.4 Study of the workability of UHPFRC for the different fiber contents

The workability of UHPFRC has been investigated for different fiber contents. Therefore, the workability of specimens without fibers, as well as with 3 Vol.-% and 6 Vol.-% steel fibers was measured with a flow table, following the procedure proposed by BS 1015-3:1999 [19]. The applied cone had a height of 60 mm, a top diameter of 70 mm and a bottom diameter of 100 mm. The flow cone was filled in two layers and each layer was tamped ten times with a

tamper. Then the cone was lifted, and the table was jolted 15 times at a rate of one jolt per second. The diameter of UHPFRC was determined as an average of perpendicular diameters. The result of the measurement of the workability indicated that the volume of steel fibers in the mixture affects the workability of UHPFRC. More specifically, while the flow diameter of Ultra High Performance Concrete (UHPC) without fibers was 255 mm, the respective values for the mixtures with 3 and 6 Vol.-% steel fibers were equal to 215 mm and 125 mm, respectively. These results indicate a good workability for the mixture without fibers, as well as for the mixture with 3 Vol.-%. On the contrary, the high volume of steel fibers in the mixture prepared with 6 Vol.-% caused a pronounced reduction in flow.

2.3.5 Effect of the steel fibers' content on the performance of UHPFRC

In the present study, the effect of different fiber contents on the tensile response of UHPFRC

has been investigated. Five different fiber contents were examined, namely 1 Vol.-%, 2 Vol.-

%, 3 Vol.-%, 4 Vol.-% and 6 Vol.-%. and for the preparation of the specimens cement 32.5 R

type II was used. All the examined specimens were cured in a water tank and tested at 28

193 days.

179

180

181

182

183

184

185

186

187

188

189

190

191

192

194

195

197

198

199

200

Figures 13a-e present the results of the direct tensile tests of the examined specimens with

different fiber contents, together with the average curves.

The maximum tensile strengths for the different fiber contents are illustrated by Figure 14.

From the experimental results it is evident that as the amount of steel fibers in the mixture is

increasing, the ultimate tensile strength also increases. More specifically, while the elastic

part of the tensile response is not considerably affected by the volume fraction of steel fibers,

the post-elastic strength is highly affected by the fiber volume.

In addition to the tensile tests, compressive tests with standard cubes were executed for all the examined mixtures. The compressive strengths for the different fiber contents are presented by Figure 15.

The results of Figures 14 and 15 indicate that as the steel fiber content increased, both compressive and tensile strength increased too.

2.3.6 Effect of the fiber content on the variation of experimental results

The Coefficient of Variation (CV) has been calculated for the examined mixtures with the various amounts of steel fibers and the results are presented by Figure 16.

As the amount of steel fibers increased, the CV also increased; for the highest steel fiber content (6 Vol.-%), the CV was almost twice as high as specimens with 4 Vol.-% steel fibers. As presented in the previous section, with higher percentages of steel fibers the workability is significantly reduced and subsequently this is affecting the distribution of the steel fibers in the mixture.

2.3.7 The effect of fiber content on the fracture energy

The amount of steel fibers in the mixture can affect apart from the strength, the fracture energy of UHPFRC. For this reason, and with the average tensile stress-strain curves for the different percentages of steel fibers, the fracture energy was calculated. The fracture energy has been investigated in a number of studies [20-22], for different fiber reinforced concretes, and it can be defined as the dissipated work which is necessary for the separation of two crack surfaces [20]. The fracture energy can be calculated by the following equation [20]:

221
$$G = \frac{Q}{A_f} = \frac{\int_{w=0}^{w=w_u} F_t(w) dw}{A_f}$$
 (1)

222 Where:

- 223 Q: the dissipated work needed for the generation of a crack
- 224 A_f: the new crack fracture area
- 225 F_t: the load applied in tension
- 226 w: the crack opening

234

235

236

237

238

239

240

241

242

243

- w_u: the crack opening at the stage of complete separation 227
- w_m: permanent crack opening 228
- The fracture energy can be distinguished in the energy dissipated during the strain hardening 229
- (G_a) and the strain softening (G_b) ,. 230
- The fracture energy is according to Equation 2 (Figure 17): 231

$$G=G_a+G_b \tag{2}$$

With the average stress-strain curves for the different percentages of steel fibers the fracture 232

233 energy was calculated and the results are presented in Table 3.

The results of Table 3 indicate that very high values of fracture energy can be achieved for high percentages of steel fibers. For percentages of steel fibers between 1-3 Vol.-% the fracture energy presented a minor upward trend at increasing fiber dosage. Fracture energy values equal to 24.4 KJ/m² and 28.4 KJ/m² were obtained for specimens with 4 and 6 Vol.-% steel fibers respectively. These values are in the range of reported values in the literature for similar investigations. More specifically, the fracture energy of various UHPFRC mixes has been evaluated [20-22]. Benson and Karihaloo [22] recorded a value of fracture energy equal to 20 KJ/m² using 6 Vol.-% steel fibers, while for the same percentage of steel fibers, a value of 24 KJ/m² was recorded by Habel et al. [21]. Wille and Naaman [20], conducted a research on the improvement of the fracture energy of UHPFRC, and with an optimized UHPFRC

with a compressive strength of 200 MPa they found a fracture energy which exceeded 30 KJ/m² using 1.5 Vol.-% twisted steel fibers.

2.4. Stress-Strain and Stress-Crack Opening Models for different fiber contents

246

247

248

249

250

251

252

253

254

255

256

257

258

259

260

261

262

263

264

265

266

267

The experimental results of the investigation of the effect of different fiber contents on the tensile performance and on the stress-strain response of UHPFRC, were used to model the behavior of the material in tension. The behavior of the material is divided in two parts. The parts are; first up to a maximum stress level and second after the maximum stress level is reached, when the response of the material is governed by the formation of a single crack. The direct tensile results show that the stress-strain behavior up to a maximum stress level depend on the amount of steel fibers in the mixture. Hence, for the different fiber contents, different ascending branches can be distinguished as presented by Figures 18a-c. The tensile behavior of specimens with 1 Vol.-% steel fibers is characterized by strainsoftening behavior and the initial response is simulated with one linear branch up to a maximum stress level (Figure 18a). Specimens with 2 and 3 Vol.-% steel fibers on the other hand, presented strain-hardening behavior and two branches were used to represent the stressstrain behavior up to a maximum stress level (Figure 18b). The first branch was limited to the end of the elastic state $(\sigma_{u,1}, \varepsilon_{u,1})$ and the second ended at the maximum stress $(\sigma_{u,max}, \varepsilon_{u,max})$. Finally, the incorporation of high percentages of steel fibers (4 and 6 Vol.-%) caused a pronounced strain-hardening state. Hence, a third branch $(\sigma_{u,2}, \varepsilon_{u,2})$ was inserted in the ascending branch in order to simulate the behavior of the material up to the maximum stress level (Figure 18c). The effect of the fiber content in the post-elastic state, is shown by Figure 19. In this figure, the strain-hardening of the average curves of specimens with 3, 4 and 6 Vol.-% steel fibers is presented. As shown in this figure, the strain-hardening of the specimens with 3 Vol.-% can

be represented with one branch. However, for specimens with 4 and 6 Vol.-% steel fibers, a 268 second branch in the post-elastic state can be distinguished and is required in this state to 269 model the strain-hardening of the specimens with this fiber content. 270 Similar models for the modelling of the stress-strain behavior proposed by Habel et al. [10] 271 for UHPFRC and RILEM TC 162-TDF [1] for SFRC. The experimental results of the present 272 study indicate that the responses of specimens up to a fiber content of 3 Vol.-%, are in good 273 agreement with the shape of existing models available in the literature (Habel et al. [10]). 274 However, existing models could not accurately model the response of specimens with higher 275 276 fiber contents. Therefore, in the present study, the response of mixtures with fiber contents higher than 3 Vol.%, was modelled with a tri-linear model. The characteristic values of the 277 proposed models of Figure 18 are presented by Table 4. All the values for the elastic state 278 279 presented in Table 4 are based on the stress and strain results at the end of the initial linear part which was identified graphically. 280 In all the examined cases, in which the tensile response was characterized by a strain-281 hardening behavior (2-6 Vol.-%), the second modulus elasticity (E_{U.hard}) was calculated. This 282 can be defined as the ratio of the stress to strain in the hardening state (Figures 18b and 18c). 283 From the calculation of the second modulus of elasticity, it was evident that as the volume 284 fraction of the fibers increased the second modulus of elasticity also increased. 285 286 The stress-crack opening behavior can be modelled with a bi-linear curve, as illustrated by 287 Figure 20; the obtained characteristic values are presented by Table 5. The proposed values of the present study in this state are in good agreement with the findings of other researchers 288 for similar models. Based on the model proposed by Habel et al. [10], it is considered that at 289 290 approximately half of the fiber length, no more stresses are transferred through the crack. This assumption is in good agreement with the proposed values of the current study, which 291

are based on the experimental results, and have been found to be in the range of 5.3-6.6 mm, for a fiber length of 13 mm.

2.5. Existing models for the modeling of the tensile behavior of UHPFRC

292

293

294

295

296

297

298

299

300

301

302

303

304

305

306

307

308

309

310

311

312

313

314

315

The fiber content is crucial for the tensile characteristics of UHPFRC after the formation of the first cracks. According to AFGC-SETRA [23], three different types of tensile behavior can be distinguished for UHPFRC. The first type is a strain-softening behavior (Figure 21a), the second is a low strain-hardening behavior (Figure 21b), and the third is a high strainhardening behavior (Figure 21c). In case of strain-softening (Figure 21a), the ultimate strength of UHPFRC is equal to the strength of the concrete matrix. In cases of low and high strain-hardening the post-cracking resistance of UHPFRC is higher than the resistance of matrix. However, for different fiber contents, a different post-elastic behavior can be distinguished. Based on the experimental results of the present research, for fiber contents higher than 4 Vol.-%, there is a clear difference on the tensile response of the mixture compared to the respective results prepared with fiber contents 2 and 3 Vol.-%. More specifically, in case of 2 and 3 Vol.-% fibers, and based on the results of Table 4, the ratio $\frac{E_{u,hard}}{E_{v,l}}$ was found equal to 4%, while for the mixtures with 4 and 6 Vol.-% steel fibers the respective ratio was found equal to 28% and 40%. This indicates a clearly enhanced post elastic state for the mixtures with 4 and 6 Vol.-%, which is defined as 'high-strain' hardening behavior. Consequently, specimens with 2 and 3 Vol.-% steel fibers can be defined as "low strain-hardening" UHPFRCs (Figure 21b) and two branches are required to represent the stress-strain behavior up to a maximum stress level (Figure 18b). Specimens with 4 and 6 Vol.-% can be defined as "high strain-hardening" UHPFRCs (Figure 21c) and a tri-linear model is required for the modelling of the tensile behavior (Figure 18c). -

3. Discussion

316

317

318

319

320

321

322

323

324

325

326

327

328

329

330

331

332

333

In the present study, the tensile and compressive behavior of UHPFRC were investigated for different curing regimes and different mixture compositions. The effect of different cement types was also examined. The experimental results indicated that the use of high strength cement can increase both the tensile and the compressive strengths of UHPFRC. Direct tensile and compressive tests were conducted on a number of specimens that contained different fiber contents. Based on the experimental results, it was evident that the steel fiber content in the mixture affected the compressive strength, the tensile characteristics and the fracture energy of the material. Therefore, different models, depending on the fiber content, are required for the modelling of the material in tension. However, an aspect which should be taken into consideration is that the big volume of fibers in the mixture (higher than 3 Vol.-%), has a negative effect on the workability of the mixture. In this case, the good rheological properties of UHPFRC should be secured, with higher water/cement ratio or the use of higher quantity of superplactiser. From the study of different curing regimes on the mechanical properties of UHPFRC, the effectiveness of the heat curing was proved and it accelerated the strength development. However, heat curing for more than 12 days is not suggested as it has not any further effect on the strength development.

4. Conclusions

- From the results of the present study the following conclusions can be drawn:
- The use of 52.5 N type I cement instead of 32.5 R type II cement resulted in 18% higher
- tensile strength and 16% higher compressive strength.
- The increase of the fiber content from 1 to 6 Vol.-% increased the tensile strength by 92%
- and the compressive strength by 72%.

- Specimens with 1 Vol.-% steel fibers presented a strain-softening behavior; strain hardening 339 was achieved with a fiber dosage of at least 2 Vol.-%. 340 • The stress-strain response of specimens with 1 Vol.-%, up to the maximum stress level, was 341 simulated with one linear branch. 342 • Specimens with 2 and 3 Vol.-% steel fibers presented a low strain-hardening behavior and a 343 bi-linear model was used for the simulation of their response up to the maximum stress level. 344 • Specimens with 4 and 6 Vol.-% steel fibers presented a high strain-hardening behavior and a 345 tri-linear model was used for the simulation of their response up to the maximum stress level. 346 347 • The stress-crack opening behavior in all the examined cases was simulated with a bi-linear model. 348 • High values of fracture energy were achieved for specimens with high strain-hardening 349 350 behavior in tension. Therefore, the fracture energy of the mixture with 4 Vol.-% was found to be equal to 24.4 KJ/m², while for specimens with 6 Vol.-% steel fibers was equal to 28.4 351 KJ/m^2 . 352 • From the investigation of the different curing regimes and the curing period, it was observed 353
- that the 7 days strength of the steam-cured specimens was almost the same as the 90 days strength of the specimens cured under normal conditions.
- The optimum properties of UHPFRC were achieved for steam-curing for 12 days.
- The Coefficient of Variation (CV) increased at increasing fiber content. Regarding the effect of curing time, it was found that the CV was lower for a longer curing of UHPFRC in the steam curing tank.

Acknowledgements 360 The authors would like to express their gratitude to David Pope for his assistance during the 361 362 testing, and they would also like to acknowledge Sika Limited and Hanson Heidelberg Cement Group for providing raw materials. 363 **Notation** 364 $\varepsilon_{u,1}$: strain at the end of the linear part 365 $\varepsilon_{u,2}$: strain at the end of the second branch of the proposed stress-strain model for high strain 366 hardening behavior 367 $\varepsilon_{u,max}$: strain at the maximum load 368 w: the crack opening 369 w_{u,1}: crack opening at the end of the descending part of the proposed stress-crack opening 370 371 model w_{u,2}: maximum crack opening 372 w_u: the crack opening up to the complete separation 373 w_m: permanent crack opening 374 $\sigma_{u,1}$: stress at the end of the elastic part 375 $\sigma_{u,2}$: stress at the end of the second branch of the proposed stress-strain model for high strain 376 377 hardening behavior $\sigma_{u,max}$: stress at the maximum load 378

379	σ_1 : stress at the end of the first linear part of the descending stress-crack opening model
380	Eu: modulus of elasticity
381	E _{u, hard} : second modulus of elasticity
382	Q: the dissipated work needed for the generation of a crack
383	A _f : the crack fracture area
384	F _t : the load applied in tension
385	G: the fracture energy
386	Ga: energy dissipated during the strain-hardening phase
387	G _b : energy dissipated during the strain-softening phase
388	l_{f} : length of the steel fibers
389	
390	
391	References:
392	[1] RILEM TC 162-TDF, Test and design methods for steel fiber reinforced concrete-Design
393	of steel fiber reinforced concrete using the σ -w method: principles and applications, Materials
394	and Structures, 35: (2002), 75-81.
395	[2] Nicolaides D., Kanellopoulos A., Petrou M., Savva P., Mina A., Development of a new
396	Ultra High Performance Fiber Reinforced Cementitious Composite (UHPFRCC) for impact
397	and blast protection of structures, Construction and Building Materials, 95: (2015), 667-674.

- 398 [3] Kang S.T., Lee Y., Park Y.D., Kim J.K., Tensile fracture properties of an Ultra High
- 399 Performance Fiber Reinforced Concrete (UHPFRC) with steel fibers, Composite Structures,
- 400 92 (1): (2010), 61-71.
- 401 [4] Yoo Y., Shin H.O., Yang J.M., Yoon Y.S., Material and bond properties of Ultra High
- 402 Performance Fiber Reinforced Concrete with micro steel fibers, Composites Part B:
- 403 Engineering, 58: (2013), 122-133.
- 404 [5] Neocleous K., Tlemat H., Pilakoutas K., Design issues for concrete reinforced with steel
- 405 fibers including fibers recovered from used tires, Journal of Materials in Civil Engineering
- 406 ASCE, 18 (5): (2006), 677 685.
- 407 [6] Kooiman A.G., Van der Veen C., Walraven. J.C., Modelling the post-cracking behavior
- of steel fiber reinforced concrete for structural purposes, HERON, 45: (2000), 275-307.
- 409 [7] Kang S.T., Kim J.K., The relation between fiber orientation and tensile behavior in an
- 410 Ultra High Performance Fiber Reinforced Cementitious Composites (UHPFRCC), Cement
- and Concrete Research, 41(10): (2011), 1001-1014.
- 412 [8] Ferrara L, Ozyurt N, Di Prisco M., High mechanical performance of fiber reinforced
- 413 cementitious composites: the role of "casting-flow induced" fiber orientation, Materials and
- 414 Structures, 44 (1): (2011), 109-128.
- [9] Paschalis S, Lampropoulos A., Size effect on the flexural Performance of UHPFRC,
- 416 Proceedings of the 7th HPFRCC Conference, Stuttgart, Germany, 1-3 June 2015.
- 417 [10] Habel K., Denarie E., Bruhwiler E., Structural response of elements combining Ultra
- 418 High Performance Fiber Reinforced Concretes and Reinforced Concrete. Journal of
- 419 Structural Engineering, 132 (11): (2006), 1793-1800.
- 420 [11] Paschalis S., Lampropoulos A., Ultra High Performance Fiber Reinforced Concrete
- 421 Under Cyclic Loading, ACI Materials Journal, 113 (4): (2016), 419-427.

- 422 [12] Lampropoulos A., Paschalis S., Tsioulou O., Dritsos S., Strengthening of reinforced
- 423 concrete beams using Ultra-High Performance Fiber-Reinforced concrete (UHPFRC),
- 424 Engineering Structures, 106: (2015), 370-384.
- 425 [13] Lampropoulos A., Paschalis S., Tsioulou O., Dritsos S., Strengthening of existing
- 426 reinforced concrete beams using Ultra High Performance Fiber Reinforced Concrete
- 427 (UHPFRC), Concrete Repair, Rehabilitation and Retrofitting IV, Leipzig, Germany, 5-7
- 428 October 2015.
- 429 [14] Lampropoulos A., Paschalis S., Dritsos S., UHPFRC vs RC jackets for the seismic
- 430 upgrade of columns Structural Engineering: Providing Solutions to Global Challenges,
- 431 IABSE, International Conference Centre Geneva, Geneva, Switzerland, 23-25 September
- 432 2015.
- 433 [15] Hassan A., Jones S., Mahmud G., Experimental test methods to determine the uniaxial
- 434 tensile and compressive behavior of Ultra High Performance Fiber Reinforced Concrete
- 435 (UHPFRC), Construction and Building Materials, 37: (2012), 874-882.
- 436 [16] BS EN 12390-3:2009, Testing hardened concrete-Part 3: Compressive strength of test
- 437 specimens
- 438 [17] Benson S.D.P, CARDIFRC-Development and constitutive behavior, PhD Thesis,
- 439 Cardiff, Cardiff University, 2003.
- [18] Karihaloo B.L., Benson S.D.P., Alaee, F.J., CARDIFRC UK pattern GB2391010 (2005).
- 441 [19] BS EN 1015-3:1999, Methods of test for mortar for masonry-Part 3: Determination of
- consistence of fresh mortar (by flow table).
- 443 [20] Wille K., Naaman A.E., Fracture energy of UHP-FRC under direct tensile loading,
- Proceedings of Fracture Mechanics of Concrete and Concrete Structures-Recent Advances in
- 445 Fracture Mechanics of Concrete-7, Seoul, South Korea, 23-28 May 2010.

446	[21] Habel K., Viviani M., Denarie E., Bruehwiler E., Development of the mechanical
447	properties of an Ultra-High Performance Fiber Reinforced Concrete (UHPFRC), Cement and
448	Concrete Research, 36 (7): (2006), 1362-1370.
449	[22] Benson S.D.P, Karihaloo B.L., CARDIFRC-Development and mechanical properties,
450	Part III: Uniaxial tensile response and other mechanical properties, Magazine of Concrete
451	Research, 57 (8): (2005), 433-443.
452	[23] AFGC-SETRA 2013, Ultra High Performance Fiber Reinforced Concrete, Interim
453	Recommendations, SETRA, Bagneux, France.
454	
455	
456	
457	